A cooperative domain model for multiple phase transitions and complex conformational relaxations in polymer with shape memory effect

Haibao Lu[1,3], Xiaodong Wang[1], Ziyu Xing[1] and Yong-Qing Fu[2]

[1]National Key Laboratory of Science and Technology on Advanced Composites in Special Environments Laboratory, Harbin Institute of Technology, Harbin 150080, China

[2]Faculty of Engineering and Environment, Northumbria University, Newcastle upon Tyne, NE1 8ST, UK

[3]E-mail: luhb@hit.edu.cn

Abstract: Shape memory polymers (SMPs) are thermo-rheologically complex materials showing significant temperature and time dependences. Their segments often undergo cooperative phase transitions and conformational relaxations simultaneously along with shape memory effect (SME). In this study, a cooperative domain model is proposed to describe the composition dependence, multiple phase transitions and conformational relaxations of SMPs within their glass transition zones. Variations in local-area compositions and cooperative domains of the amorphous SMPs cause significant differences in their segmental relaxation. At a fixed domain size, both intermolecular activation energy and relaxation time significantly influence the SME and thermomechanical properties of the SMPs. Finally, the model is successfully applied to predict the shape memory behavior of SMPs with one stage SME and triple-SME, and the theoretical results have been validated by the experimental ones. This model could be a powerful tool to understand the working mechanisms and provide a theoretical guidance for the designs of multi-SME in SMPs.

Keywords: Conformational relaxation, shape memory polymer, cooperative, model

1. Introduction

Shape memory polymers (SMPs) are one of the most popular smart materials which can recover from their temporary shapes and memorize their original shapes upon receiving a suitable environmental stimulus, including heat, light, electricity, solvent, or magnetic field [1-5]. Different from other types of smart polymers such as elastomers [6] and hydrogels [7], the SMPs have their unique shape memory effect (SME) because of the combination of a reversible switching mechanism [8] (which exists in many amorphous or crystalline polymers [9,10]) and a unique network structure (e.g., having two segments, one is hard segment to memorize the initial conformation and the other is soft one to undergo the phase transition in response to external stimulus [11]). The working mechanism of the SME in SMP has been previously investigated based on phase transition theory [12]. It is generally agreed that the SME is originated from the reversible conformational relaxation of the segments from frozen phases into active ones during the phase transition [12], thus resulting in release of the stored strain energy in the frozen segments [13].

SMPs with the triple-SME, e.g., the polymers with a capability of memorizing two temporary shapes, were firstly developed by Lendlein's group in 2006 [14]. The intrinsic working mechanism of the triple-SME is similar to that of the SME in a standard SMP, while the key difference is the distinct thermal transitions among different phases [15]. A typical SMP with the triple-SME has a two-stage thermal transition that can be utilized to maintain two independent and temporary shapes [16]. Previously Wang et al proposed a theoretical model for temperature memory effect to

characterize the multiple shape memory behaviors and multi-SME in SMPs [17]. Xie proposed another model using the stored mechanical energy to explain that the well-separated thermal transitions play a key role in design of multi-SME in SMPs [18]. However, these models are phenomenal approaches and are applicable to characterize the experimental results. The thermodynamics of the multiple phase transitions and complex conformational relaxations for the multi-SME have seldom been studied [19,20]. The unique change of the conformational entropy, which is the driving force for the multi-SME in the SMP, has not been thoroughly investigated. Therefore, it is critical to propose a theoretical model for linking the multiple phase transitions and conformational relaxations, in order to understand the working mechanism and thermodynamics in the multi-SME and then suitably design the multiple shape transition behaviors of SMPs.

In the shape recovery process of SMP with multi-SME, there are more than three types of segments undergoing relaxation simultaneously. Here the cooperative domain is defined as a group of segments (or called conformers) with the same relaxation time, and the number of the segments is described using domain size (z) [21-24]. T_0 and T^* are the low-temperature limit and high-temperature limit for the cooperative domain, respectively [21]. At the low-temperature limit (T_0), all the conformers become contacted with each other, and the entire polymer becomes a large domain. The number of conformers in one domain is nearly infinite. Whereas at the high-temperature limit (T^*), the conformers are sufficiently separated apart from each other, thus each conformer can relax independently from its neighbors. Therefore, the

number of conformers in each domain is $z=1$. When the temperature is near the glass transition temperature (T_g), the change of conformational entropy (or the change of domain size) is the driving force to trigger the phase transition [22]. For the SMP with the multi-SME, the polymer is assumed to be composed of multiple phases with different domain sizes. Each domain relaxes following its the cooperative domain model, and the molecular segments in a domain relax together as is shown in figure 1.

[Figure 1]

2. Modelling of SMP by domain size near T_g

2.1 Free strain recovery behavior

When the temperature of SMP is heated close to T_g, the frozen phase would be transformed into the active one, thus triggering the SME based on the phase transition theory [11]. The stored mechanical energy is then released during phase transition due to the entropic changes [25]. For 1 mol conformers in the SMP, the conformational entropy S_c can be therefore written as [26],

$$S_c = N_z k_B \ln c_1 \tag{1}$$

where N_z is the number of domains for 1 mol conformers, k_B is Boltzmann constant and c_1 is the conformational numbers of the conformer. The conformers in one domain are grouped together and undergo thermal transitions cooperatively. Therefore, the conformational number of the conformers in one domain is assumed to be the same value [22].

The relationship between the domain size (z) and the domain number (N_z) of the 1mol conformers can be written as follows,

$$z = N_A / N_z \tag{2}$$

where N_A is Avogadro's number.

According to the theory of domain distribution for conformers [21,27], the activation energy which is needed to trigger the frozen conformers into the active ones is determined by the domain size (z). With an increase in temperature, the domain size (z) is decreased, and the conformational entropy is increased accordingly. By substituting equation (2) into equation (1), a constitutive relationship between the domain size (z) and conformational entropy (S_c) can be obtained:

$$z = N_A k_B \ln c_1 / S_c \tag{3}$$

Now, we can define s^* as the maximum value of conformational entropy of 1 mol conformers which are not mutually restricted by each other at the temperature of T^* [22]. This will result into z =1. Therefore, s^* can be written based on the form of equation (1):

$$s^* = N_A k_B \ln c_1 \tag{4}$$

Assuming that the free energy, enthalpy and entropy of the conformers can be expressed using the parameter of s^*, we can obtain [21]:

$$\frac{S_c}{s^*} = \frac{T^*}{T^* - T_0} \cdot \frac{T - T_0}{T} \tag{5}$$

where T_0 is defined as the temperature where all the conformers are involved into one domain and the conformation entropy is at its minimum value.

Substituting equation (4) into equation (3) and then comparing with equation (5), we can obtain the following equation:

$$z(T) = \frac{s^*}{S_c} = \frac{T^* - T_0}{T^*} \cdot \frac{T}{T - T_0} \tag{6}$$

Figure 2 plots the numerical results of the domain size (z) as a function of temperature (T) while T^*=773 K and T_0=100 K (or T_0=150 K, T_0=200 K, T_0=225K or T_0=250 K, respectively). Results show that the T_0 has a strong influence on the domain size, which is increased from 1.25 to 2.82 with an increase in the T_0 from 100 K to 250 K. The simulation results also confirm that the domain size (z) of the conformers is gradually decreased from 1.25 to 1.00 with an increase in the ambient temperature from 330 K to 780 K at a given T_0 value of 100 K, due to the increases in the number of domain (N_z) and conformational entropy (S_c).

[Figure 2]

For the domain with a size of z, each conformer inside has the same activation energy ($\Delta\mu$) and the domain size is specified by the number z of conformers. The intermolecular activation energy of the domain is z times of the activation energy ($\Delta\mu$) for one conformer to relax [28], therefore, we can obtain an expression of the activation energy of the domains using their domain sizes, e.g.,:

$$\Delta H = z \cdot \Delta\mu = \left(\frac{T^* - T_0}{T^*} \cdot \frac{T}{T - T_0} \right) \cdot \Delta\mu \tag{7}$$

The conformational entropy plays an essential role to trigger the phase transition of SMP in the free recovery process, while the transition ratio (γ) is determined by the Eyring equation according to the following relationship [29]:

$$\gamma = AT \exp\left(\frac{-\Delta H}{RT} + \left(\frac{T_h - T}{b \cdot T_h - T} \right) \right) \tag{8}$$

where A is an exponential coefficient [29], T_h is the transition temperature, b is

a given constant and R ($R = 8.314 J/(mol \cdot K)$) is the gas constant.

Combining equation (7) into equation (8), we can get:

$$\gamma = AT \exp\left(-\frac{\frac{T^* - T_0}{T^*} \cdot \frac{T}{T - T_0} \Delta\mu}{RT} + \left(\frac{T_h - T}{b \cdot T_h - T} \right) \right) \tag{9}$$

Here the volume fraction of frozen phase (ϕ_f) is introduced to substitute the parameter $\varepsilon(T)/\varepsilon_{pre}$, where $\varepsilon(T)$ is the strain at temperature T, and ε_{pre} is the pre-loading strain. Therefore, equation (9) can be rewritten as:

$$\frac{\varepsilon(T)}{\varepsilon_{pre}} = \phi_f = 1 - \gamma = 1 - AT \exp\left(-\frac{T^* - T_0}{RT^*} \cdot \frac{\Delta\mu}{T - T_0} + \left(\frac{T_h - T}{b \cdot T_h - T} \right) \right) \tag{10}$$

The experimental data [11] of the dimensionless recovery strain are used to compare with the simulation results as shown in figure 3. The constants used in the equation (10) are listed in table 1. It is found that the simulation results fit well with the experimental data. According to the phase transition theory [11], there are glass transitions of the conformers with an increase in the temperature, and thus there is a significant decrease in dimensionless recovery strain. As revealed by the simulation results, the recovery strain is gradually decreased from 1.00 to 0.00 with an increase in the ambient temperature from 310 *K* to 354 *K*, and this decrease ratio becomes much larger during the glass transition stage, e.g., in the temperature range from 330 *K* to 350 *K*.

[Table 1]

[Figure 3]

To further investigate the influence of T_0 on the activation energy as a function of

temperature (T), the simulation curves (where T_0 =260 K, 270 K, 280 K, 290 K and 300 K) are plotted in figure 4(a). With the decrease of T_0 from 300 K to 260 K, the activation energy is decreased accordingly from 4297.7 KJ/mol to 2418.8 KJ/mol, with the T_g = 343 K. The simulation results in figure 4(a) reveal that the activation energy is critically determined by the value of T_0, at which the domain size z =1. On the other hand, the influence of T_0 on the recovery strain as a function of ambient temperature is shown in figure 4(b). These numerical results are presented to characterize the effect of temperature on the conformational relaxation, which is the key thermodynamic parameter and triggers the strain recovery of the polymer. It is also needed to mention that conformational relaxation and recovery strain are corresponding to the thermodynamic behaviors of the polymer at the micro-scale and macro-scale, respectively. With an increase in the ambient temperature, the polymer is recovered back to the original shape from the deformed temporary shape. It is revealed that the polymer recovers to its original shape at the ambient temperature of 279 K, 289 K, 297.9 K, 307.3 K and 316.9 K when the T_0 is increased from 260 K, 270 K, 280 K, 290 K to 300 K, respectively.

[Figure 4]

2.2 Thermomechanical properties of SMPs

For the polymer macromolecules incorporated of two, three or more than three segments, it is always assumed that the storage modulus of the SMP is proportional to the storage modulus and volume fraction of each segment [27]. Therefore, the storage modulus of the SMP with two segments can be obtained by those of the frozen phase

and active one, which can be expressed as follows:

$$\begin{cases} 1/E(T) = \phi_f/E_f + (1-\phi_f)/E_a = \left(1 - AT\exp\left(-\dfrac{T^* - T_0}{RT^*}\cdot\dfrac{\Delta\mu}{T-T_0} + \left(\dfrac{T_h - T}{b\cdot T_h - T}\right)\right)\right)/E_f \\ + AT\exp\left(-\dfrac{T^* - T_0}{RT^*}\cdot\dfrac{\Delta\mu}{T-T_0} + \left(\dfrac{T_h - T}{b\cdot T_h - T}\right)\right)/E_a \end{cases} \quad (11)$$

where E_f and E_a are the storage moduli of frozen phase and active one, respectively.

To verify the equation (11), the analysis results have been plotted in figure 5, together with the experimental data of dynamic mechanical analysis (DMA) measurement of SMP with T_g =340.78 *K* [29]. The same parameters listed in Table 1 were also used to predict the storage moduli of the same SMPs, and the simulation and experimental results of recovery strains have been plotted in figure 3. It is clearly seen that the simulation results are in good agreements with the experimental ones. With an increase in the ambient temperature from 331 *K* to 355 *K*, transition of the frozen phase into active one is accelerated, and thus the storage modulus of the SMP is decreased from 270 MPa to 20 MPa. Meanwhile, the simulation results can also be well explained using the phase transition theory [11,12], e.g., the conformational entropy of the conformers is increased with an increase in the ambient temperature, thus causing the decrease in domain size (*z*). With the domain size is decreased, both the activation energy and transition ratio are increased, while the volume fraction of frozen phase (ϕ_f) and storage modulus are both decreased, according to the equations (7), (8), (10) and (11). It should be noted that the simulation results in equation (11) are more suitable for predicting the phase transition of the SMP.

[Figure 5]

On the other hand, relaxation time (λ) is another key parameter to determine the thermomechanical properties of SMPs. The relationship between the relaxation time λ and domain size near T_g can be expressed using [21]:

$$\ln(\lambda / \lambda^*) = \frac{\Delta E}{R}(\frac{z}{T} - \frac{1}{T^*}) \tag{12}$$

where λ^* is the relaxation time at the temperature of T^*, and ΔE is the internal energy of the conformers in the domain.

When being heated to T_g, the SMP experiences the SME which is driven by the conformational relaxation of the conformers, and the internal energy of the conformers can be obtained from the activation energy as presented in equation (13):

$$\Delta E = TS_c = \Delta H - RT\left(\frac{T_h - T}{b \cdot T_h - T}\right) = \left(\frac{T^* - T_0}{T^*} \cdot \frac{T}{T - T_0}\right) \cdot \Delta\mu - RT\left(\frac{T_h - T}{b \cdot T_h - T}\right) \tag{13}$$

where $RT\left(\frac{T_h - T}{b \cdot T_h - T}\right)$ is introduced to describe the effect of internal stress on the thermomechanical properties of the SMP [22].

Combining equations (6), (12) and (13), we can obtain:

$$\ln(\lambda / \lambda^*) = \left(\left(\frac{T^* - T_0}{T^*} \cdot \frac{T}{T - T_0}\right) \cdot \frac{\Delta\mu}{R} - T\left(\frac{T_h - T}{b \cdot T_h - T}\right)\right)\left(\frac{T^* - T_0}{T^*} \cdot \frac{1}{T - T_0} - \frac{1}{T^*}\right) \tag{14}$$

Furthermore, effects of domain size and internal stress on relaxation time of the SMP were studied, where the used parameters are listed in table 1. As shown in figure 6(a), the relaxation time of the SMP is increased from 10 to 80 with an increase in the T_0 from 240.0 *K* to 250.0 *K*. With a higher value of T_0, the activation energy of the SMP becomes smaller when it is heated to a given ambient temperature, thus causing the relaxation time to be increased.

On the other hand, figure 6(a) plots the simulation curves for the effects of internal stress on the relaxation time of SMP. It is revealed that the relaxation time is gradually increased from 42 to 120 with an increase in the parameter *b* from 1.02 to 1.10. As the *b* value is increased to a higher value, the internal stress is therefore decreased to a lower value thus resulting in a longer relaxation time. These numerical results are in well agreements with the previous study [22] which reported that the internal stress has a strong effect on the relaxation time of the polymeric materials. It has been proved that a large internal stress is helpful for the polymer macromolecules to relax during the glass transition process.

[Figure 6]

3. Modelling of multi-SME near T_g using domain size

3.1 Free strain recovery behavior of SMP with multi-SME

In the previous sections, shape memory behavior and thermomechanical properties of the SMP have been well investigated and predicted using the model of domain size. It is essential to further study more complex multi-SMEs of the SMPs, of which both the shape memory behavior and thermomechanical properties are resulted from the multiple phase transitions. Each domain size is correspondent to a transition temperature which indicates that the SMPs with multiple domain sizes will have multiple phase transition temperatures or multi-SMEs. The volume fraction of frozen phases is resulted from the superposition of each frozen phase and has the following expression:

$$\phi_f = \sum_{i=1}^{n} \phi_f(i) \tag{15}$$

where n is the number of frozen phase near to the T_g, and $\phi_f(i)$ is the frozen volume fraction of the ith frozen phase.

Incorporating equation (15) into equation (10), the dimensionless recovery strain for the SMP with multi-SME can be described as follows:

$$\begin{aligned}\frac{\varepsilon(T)}{\varepsilon_{pre}} &= \sum_{i=1}^{n} \varepsilon(i)_{pre}\phi_f(i) \\ &= \sum_{i=1}^{n} \frac{\varepsilon(i)_{pre}}{\varepsilon_{pre}}\left[1 - A(i)T\exp\left(-\frac{T^* - T_0(i)}{RT^*}\cdot\frac{\Delta\mu(i)}{T - T_0(i)} + \left(\frac{T_h(i) - T}{b(i)\cdot T_h(i) - T}\right)\right)\right]\end{aligned} \tag{16}$$

where $\varepsilon(i)_{pre}$ is the pre-loading strain of the ith phase, $A(i)$, $T_0(i)$, $\Delta\mu(i)$, $T_h(i)$ and $b(i)$ are the parameters of the ith phase.

The simulation results of equation (16) have been plotted in figure 7 to compare with the experimental data [18] of the SMP with triple-SME, while the corresponding parameters used in the equation are listed in table 2. Based on figure 7, the simulation results fit well with the experimental ones. A clear two-stage recovery of strain (e.g., the first stage of transition is in the relaxation time from 0 min to 10 min, while the second one is in the relaxation time from 28 min to 47 min) has been predicted using the constitutive model which identifies the relationship between the recovery strain with the temperature and time parameters. It should be noted that the model is more suitable to characterize and predict the thermodynamic behavior of the SMP during the glass transition.

[Table 2]

[Figure 7]

3.2 Thermomechanical properties of SMP with multi-SME

To further verify the model of domain size for the SMPs with multi-SME, the thermomechanical properties were further investigated to explore the working mechanism and constitutive relationship of the SMPs. In the shape recovery process, the increase in temperature results in an obvious decrease in the storage modulus of the SMP [30]. However, so far, there are few studies on the thermomechanical properties during the multi-SMEs, of which the SMP undergoes multiple shape memory behaviors in the thermomechanical process.

For the SMPs with the multi-SMEs, the polymers are always incorporated with one hard segment and multiple soft segments. According to the thermomechanical properties of SMP, it is assumed that each soft segment is able to undergo the phase transition from the frozen state to active state. Therefore, the storage modulus as a function of temperature of the soft segment in the SMP is also determined by the equation (11). Therefore, the storage modulus of the polymer is resulted from the soft segments [29] and can be expressed as,

$$E(T) = \frac{1}{\sum_{i=1}^{n} \frac{\phi_i}{E_f(i)\phi_f(i) + E_a(i)(1-\phi_f(i))}} \tag{17}$$

where ϕ_i is the proportion of the i th segment.

Substituting equation (11) into equation (17), we can obtain the constitutive relationship for the storage modulus as a function of temperature:

$$E(T)=\frac{1}{\sum_{i=1}^{n}\phi_i\left[\begin{array}{l}\left(1-A(i)T\exp\left(-\dfrac{T^*-T_0(i)}{RT^*}\cdot\dfrac{\Delta\mu(i)}{T-T_0(i)}+\left(\dfrac{T_h(i)-T}{b(i)\cdot T_h(i)-T}\right)\right)\right)/E_f(i)\\ +A(i)T\exp\left(-\dfrac{T^*-T_0(i)}{RT^*}\cdot\dfrac{\Delta\mu(i)}{T-T_0(i)}+\left(\dfrac{T_h(i)-T}{b(i)\cdot T_h(i)-T}\right)\right)/E_a(i)\end{array}\right]} \quad (18)$$

Here equation (18) is utilized to characterize the storage moduli of the SMPs with triple-SME and then to compare with the experimental data [31] for verification. The comparison has been presented in figure 8, and the corresponding parameters used in the calculation are listed in table 3. It is revealed that the simulation results are in a good agreement with the experimental ones. The simulation results of the proposed model present a two-phase transition at different temperature ranges of (1) 300°C to 325°C; and (2) 340°C to 375°C, respectively, during which the temperature dependent storage moduli ($\log E(T)$) are decreased from 3.25 to 0.75. Results show that it is difficult to identify the two-phase transitions if the transition temperature ranges of the segments are too close between each other. The occurrence of the multi-SME is strongly dependent upon the temperature differences of each soft segment. The numerical analysis results prove that the proposed model is suitable to describe the thermomechanical properties of the SMP with multi-SME.

[Table 3]

[Figure 8]

4. Conclusion

In this study, a cooperative domain model was proposed to describe the unique characteristics of the conformational relaxations and dynamic phase transitions of the multiple segments in the SMP with multi-SMEs. Both the shape memory behavior

and thermomechanical properties of the SMP have been investigated to verify the proposed model and simulation results. Effects of the composition dependence, phase transition and conformational relaxation on the recovery strains and storage moduli were systematically studied. The constitutive relationships among domain size, activation energy and relaxation time of the SMP have formulated and discussed around the glass transition region. The model has then applied to the SMP with triple-SME, and the results have demonstrated that it can successfully describe their strain recovery and thermomechanical behaviors. From the numerical analysis of our proposed model, it provides a design principle for the multi-SME in SMPs. This study is expected to provide a powerful tool to understand the working mechanism and provide a theoretical guidance for the design of multi-SME in SMPs.

Acknowledgements

This work was financially supported by the National Natural Science Foundation of China (NSFC) under Grant No. 11672342 and 11725208, Newton Mobility Grant (IE161019) through Royal Society and NFSC.

Reference

[1] Mather P T, Luo X F and Rousseau I A 2009 *Annu. Rev. Mater. Res.* **39** 445-71

[2] Lu H B, Yao Y T, Huang W M and Hui D 2014 *Compos. B. Eng.* **67** 290-5

[3] Lendlein A, Jiang H, Junger O and Langer R 2005 *Nature* **434** 879-82

[4] Mohr R, Kratz K, Weigel T, Lucka G M, Moneke M and Lendlein A 2006 *Proc. Natl. Acad. Sci. USA.* **103** 3540-5

[5] Hilmar K, Gary P, Nathan A P, Max A and Richard A V 2004 *Nature. Mater.* **3** 115-20

[6] Wang Y, Ameer G A, Sheppard B J and Langer R 2002 *Nat. Biotechnol.* **20** 602-6

[7] Miyata T, Asami N and Uragami T 1999 *Nature* **399** 766-9

[8] Xie T 2011 *Polymer* **52** 4985-5000

[9] Hu J L, Zhu Y, Huang H H and Lu J 2012 *Prog. Polym. Sci.* **37** 1720-63

[10] Meng H, Mohamadian H, Stubblefield M, Jerro D, Ibekwe S and Pang S S 2013 *Smart. Mater. Struct*. **22** 093001

[11] Liu Y, Gall K, Dunn M L, Greenberg A R and Diani J 2006 *Int. J. Plast*. **22** 279-313

[12] Liu Y, Gall K, Dunn M L and Greenberg A R 2005 *MRS Proceedings* **855** 1-6

[13] Lu H B, Wang X D, Yu K, Huang W M and Yao Y T 2017 *Smart. Mater. Struct.* **26** 095011

[14] Bellin I, Kelch S, Langer R and Lendlein 2006 *Proc. Natl. Acad. Sci. USA.* **103** 18043-7

[15] Liu G Q, Ding X B, Cao Y P, Zheng Z H and Peng YX 2005 *Macromol. Rapid. Commun.* **26** 649-52

[16] Luo X F and Mather P T 2010 *Adv. Funct. Mater.* **20** 2649-56

[17] Wang Y R, Li J, Li X J, Pan Y, Zheng Z H, Ding X B and Peng Y X 2014 *Rsc. Adv.* **4** 20364

[18] Xie T 2010 *Nature* **464** 267-70

[19] Yu K, Xie T, Leng J S and Qi H J 2012 *Soft Matter* **8** 5687-95

[20] Li X J, Yang J Q, Liu C M, Bai G, Luo W B and Li P W 2018 *Microelectron.*

Reliab. **82** 130-5

[21] Matsuoka S and Quan X 2002 *Macromolecules* **24** 2770-9

[22] Matsuoka S, Quan X, Laboratories T B and Hill M 1991 *J. Non-cryst. Solids.* **133** 293-301

[23] Ngai K L and Roland C M 1993 *Macromolecules* **26** 6824-30

[24] Roland C M 1992 *Macromolecules* **25** 7031-6

[25] Lu H B, Yu K, Sun S J and Leng J S 2010 *Polym. Int.* **59** 766-71

[26] Flory P J and Krigbaum W R 1950 *J. Chem. Phys.* **18** 1086-94

[27] Adam G and Gibbs J H 1965 *J. Chem. Phys.* **43** 139-146

[28] Hodge I M 1994 *J. Non-cryst. Solids.* **169** 211-66

[29] Lu H B, Wang X D, Yao Y T and Fu Y Q 2018 *Smart. Mater. Struct.* **27** 065023

[30] Li G Q and Xu W 2011 *J. Mech. Phys. Solids.* **59** 1231-50

[31] Xie T, Xiao X and Cheng Y T 2009 *Macromol. Rapid. Commun.* **30** 1823-7

Tables caption

Table 1. Fitting data of equation (10).

Table 2. Value of parameters used in equation (16).

Table 3. Value of parameters used in equation (18).

Table 1. Fitting data of equation (10).

Parameter	A	$T^{*}(K)$	$T_0\,(K)$	$T_h\,(K)$	$\Delta\mu(KJ/mol)$	b
Value	0.058	773	308.69	355	880.5	1.01

Table 2. Value of parameters used in equation (16).

i	$\varepsilon(i)_{pre}$	$A(i)$	$T_0(i)$ (K)	$b(i)$	$T_h(i)$ (K)	$\Delta\mu(i)$ (KJ/mol)
1	0.59	0.0033	290.47	1.04	325.861	1016.5
2	0.41	0.00238	309.228	0.99	415.8159	1431.07

Table 3. Value of parameters used in equation (18).

i	$\Phi(i)$	$A(i)$	$T_0(i)$ (K)	$b(i)$	$T_h(i)$ (K)	$\Delta\mu(i)$ (KJ/mol)
1	0.45	0.00259	294.23	0.895	322.5	1000
2	0.55	0.012	319.57	0.8719	363	1000

Figures caption

Figure 1. Schematic diagram of the change of domain size with temperature near T_g.

Figure 2. Numerical results for the domain size as a function of temperature at a given T_0, where T_0 =100*K*, 150*K*, 200*K*, 225*K* and 250*K*.

Figure 3. Comparison of recovery strain between the experimental data [11] and simulation results using equation (10).

Figure 4. (a) Changes of activation energy with temperature in different domains (T_0 =280*K*, 290*K*, 300*K* and 308.7*K*). (b) Simulation results of the recovery strains with temperature T_0 =260 *K*, 270 *K*, 280 *K*, 290 *K* to 300 *K*.

Figure 5. Comparison between the simulation results and experimental data [30] of storage modulus of SMP.

Figure 6. Simulation results of relaxation as a function of temperature. (a) For the effects of domain size on the relaxation time. (b) For the effects of internal stress on the relaxation time.

Figure 7. Comparison between the simulation result of equation (16) and the experiment data [18] of the SMP with triple-SME

Figure 8. Comparison between the simulation result of equation (18) and the experimental data of SMP with triple-SME [31].

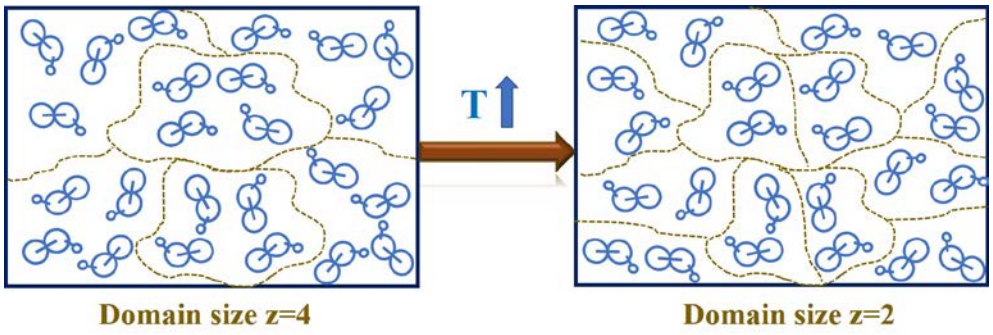

Figure 1. Schematic diagram of the change of domain size with temperature near T_g.

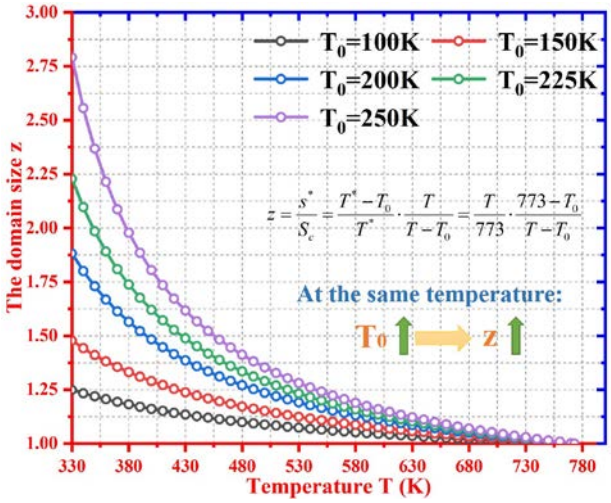

Figure 2. Numerical results for the domain size as a function of temperature at a given T_0, where T_0 =100K, 150K, 200K, 225K and 250K.

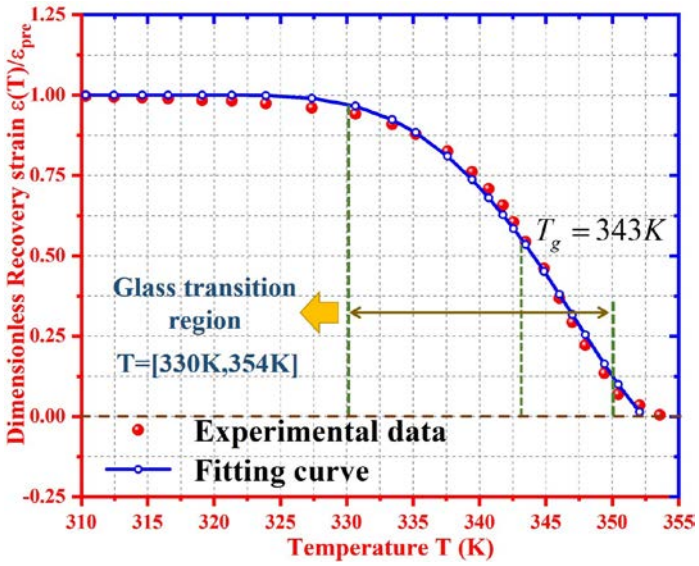

Figure 3. Comparison of recovery strain between the experimental data [11] and simulation results using equation (10).

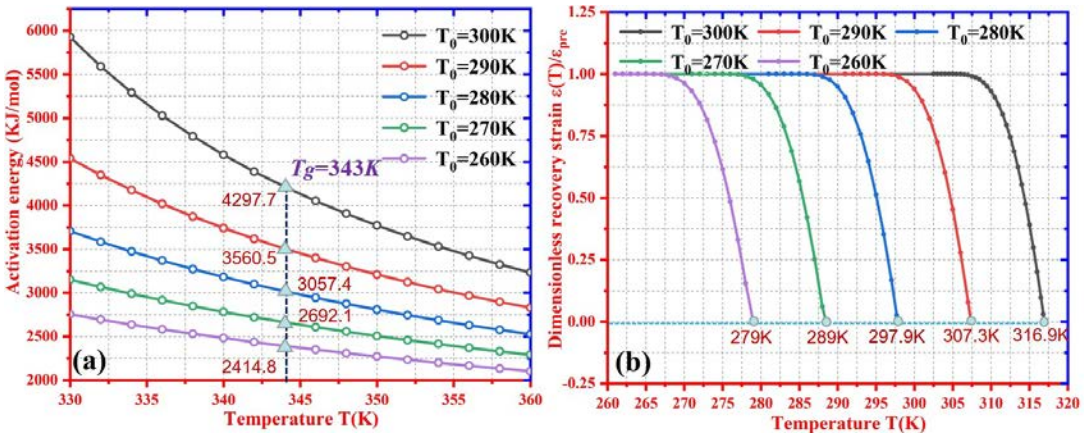

Figure 4. (a) Changes of activation energy with temperature in different domains (T_0 =280*K*, 290*K*, 300*K* and 308.7*K*). (b) Simulation results of the recovery strains with temperature T_0 =260 *K*, 270 *K*, 280 *K*, 290 *K* to 300 *K*.

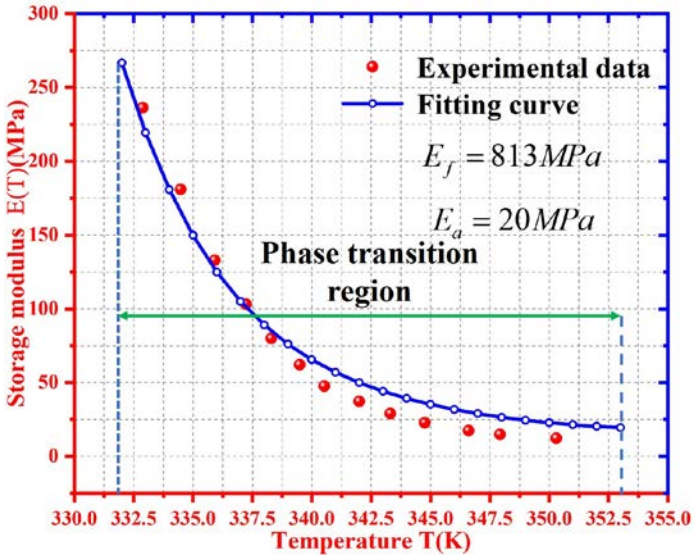

Figure 5. Comparison between the simulation results and experimental data [30] of storage modulus of SMP.

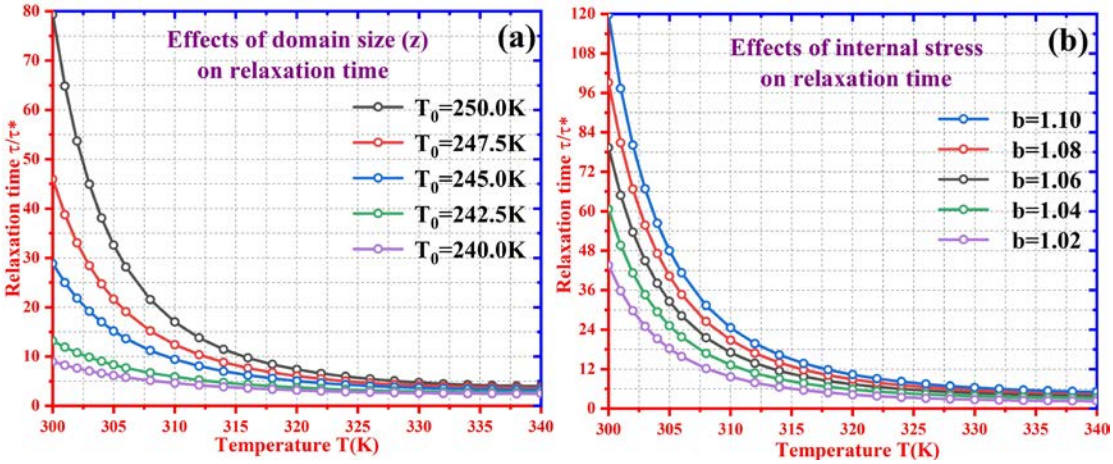

Figure 6. Simulation results of relaxation as a function of temperature. (a) For the effects of domain size on the relaxation time. (b) For the effects of internal stress on the relaxation time.

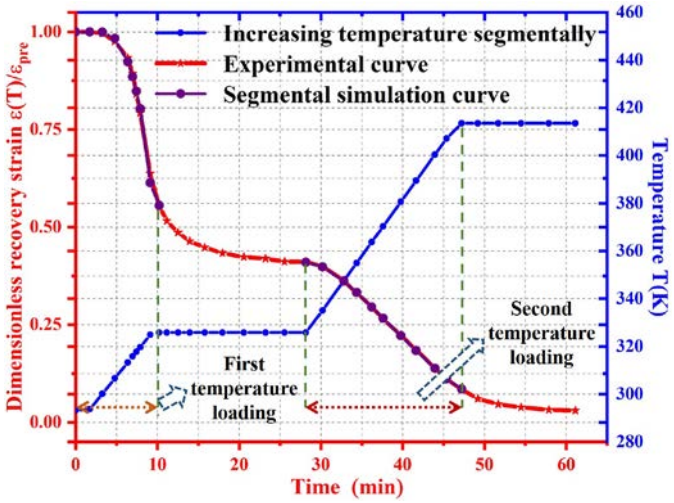

Figure 7. Comparison between the simulation result of equation (16) and the experiment data [18] of the SMP with triple-SME

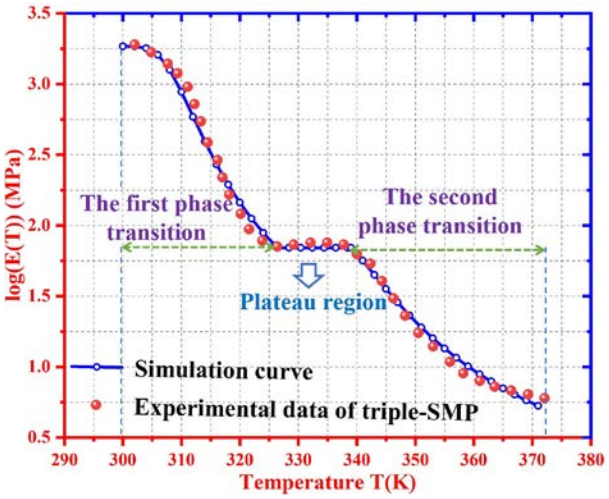

Figure 8. Comparison between the simulation result of equation (18) and the experimental data of SMP with triple-SME [31].